CHARLES UNIVERSITY IN PRAGUE

FACULTY OF PHARMACY IN HRADEC KRÁLOVÉ

Department of Pharmaceutical Chemistry and Drug Control

UNIVERSITY OF LJUBLJANA

FACULTY OF PHARMACY

Department of Medicinal Chemistry

Characterisation of Gyrase inhibitors using ITC and enzymatic assay

Diploma thesis

Charakterizace inhibitorů gyrázy s použitím ITC a enzymatického testování

Diplomová práce

Supervisors: prof. PharmDr. Martin Doležal, Ph.D.

assoc. prof. Dr. Janez Ilaš, Ph.D.

2015   Michaela Barančoková

Acknowledgements

Plagiarism statement

I declare that this thesis is my original author work. Literature and other sources used in the thesis are stated in the list of reference and cited properly. This thesis was not used to acquire any other degree.

In Hradec Králové, 15th May 2015
....

Michaela Barančoková

Abstract

Charles University in Prague, Faculty of Pharmacy in Hradec Králové

Department of Pharmaceutical Chemistry and Drug Control

University of Ljubljana, Faculty of Pharmacy

Department of Medicinal Chemistry

Supervisors: prof. PharmDr. Martin Doležal, Ph.D.

assoc. prof. Dr. Janez Ilaš, Ph.D.

Student: Michaela Barančoková

Title of Diploma Thesis: Characterisation of Gyrase inhibitors using ITC and enzymatic assay

This paper deals with *in vitro* evaluation of inhibitors of gyrase and topoisomerase IV - enzymes of type II topoisomerases family. These enzymes are essential for the proper function of bacterial cell and their inhibition leads to its destruction. The experimental part of the work had been developed at the Department of Medicinal Chemistry at the University of Ljubljana within Erasmus+ program. Tested novel inhibitors based on substituted pyrroleamide moiety with GyrB (ParE) mechanism of action were developed at the same department. The basic parameters of DNA topology, types and classification of topoisomerases, mechanism of action and structure of gyrase and topoisomerase IV and brief summary of inhibitors used in clinical practice were described. Enzymatic assay was used for evaluation in the experimental part, and half maximal inhibitory concentration IC_{50} was calculated. The activity against *E. coli* gyrase, *E. coli* topoisomerase IV*, S. aureus* gyrase and *S. aureus* topoisomerase IV was measured. Results were analyzed and described as structure-activity relationship (SAR) of given compounds. ITC (isothermal titration calorimetry) was carried out for some compounds as complementary analysis and thermodynamic characterization of binding was analyzed. Compounds KMG-15 KMG-17 and NAS-37 were evaluated as the most effective with dual targeting against all tested types of enzymes. Compounds TJL-19, TMK-16, 9-KMG and KMG-11 showed high activity against *E. coli* gyrase but were not tested against other enzymes. Further experiments will be performed in the future.

Key words: Topoisomerases, gyrase, topoisomerase IV, inhibitors, enzymatic assay, Isothermal Titration Calorimetry

Abstrakt

Univerzita Karlova v Praze, Farmaceutická fakulta v Hradci Králové

Katedra farmaceutické chemie a kontroly léčiv

University of Ljubljana, Faculty of Pharmacy

Department of Medicinal Chemistry

Školitelé: prof. PharmDr. Martin Doležal, Ph.D.

               assoc. prof. Dr. Janez Ilaš, Ph.D.

Student: Michaela Barančoková

Název diplomové práce: Charakterizace inhibitorů gyrázy s použitím ITC a enzymatického testování

Tato práce se zabývá *in vitro* hodnocením inhibitorů gyrasy a topoisomerasy IV – enzymů spadajících do rodiny topoisomeras typu II. Tyto enzymy jsou nezbytné pro správnou funkci bakteriální buňky a jejich inhibicí dochází k jejímu zániku. Experimentální část práce byla vypracována na Katedře Medicinální Chemie při Univerzitě v Lublani v rámci programu Erasmus+. Testované nové inhibitory na bázi substituovaného pyrrolamidu s GyrB (ParE) mechanismem účinku byly vyvinuty na tomtéž oddělení. Byly popsány základní parametry DNA topologie, typy a rozdělení topoisomeras, mechanismus účinku a struktura gyrasy a topoisomerasy IV a stručné shrnutí inhibitorů používaných v klinické praxi. V experimentální části byla pro hodnocení použita metoda enzymatického testování, pomocí níž byla vypočítána hodnota inhibiční koncentrace IC_{50}. Byla zjišťována aktivita proti *E. coli* gyrase, *E. coli* topoisomerase IV, *S. aureus* gyrase a *S. aureus* topoisomerase IV. Výsledné hodnoty jsou zpracovány a popsány jako vztah aktivity a účinku (SAR) daných sloučenin. Jako doplňková analýza bylo pro některé sloučeniny provedeno hodnocení pomocí ITC metody (isotermní titrační kalorimetrie), pomocí níž byl objasněn termodynamický charakter vazeb. Jako nejúčinnější byly zjištěny sloučeniny KMG-15, KMG-17 a NAS-37 s duální aktivitou proti všem testovaným typům enzymů. Sloučeniny TJL-19, TMK-16, KMG-9 a KMG-11 ukázaly vysokou účinnost proti *E. coli* gyrase, proti jiným enzymům nebyly testovány. Do budoucna je plánováno další testování.

Klíčová slova: Topoisomerasy, gyrasa, topoisomerasa IV, inhibitory, enzymatické testování, Isotermní titrační kalorimetrie

Table of Contents

Abbreviations

ADP	Adenosine diphosphate
ALL	Acute lymphoblastic leukemia
AML	Acute myeloid leukemia
ATP	Adenosine triphosphate
bp	Base pairs
BSA	Bovine serum albumin
cccDNA	Covalently closed circular DNA
Cmpd	Compound
DMSO	Dimethyl sulphoxide
DNA	Deoxyribonucleic acid
dsDNA	Double-stranded DNA
DTT	Dithiothreitol
E. coli	*Escherichia coli*
EDTA	Ethylenediaminetetraacetic acid
Em	Emission
Ex	Excitation
GyrA	Gyrase A subunit
GyrB	Gyrase B subunit
IC$_{50}$	Half maximal inhibition concentration
ITC	Isothermal titration calorimetry
Lk	Linking number
ln	Natural logarithm of *e*
mtDNA	Mitochondrial DNA
MW	Molecular weight
NOVOB	novobiocin
ParC	Topoisomerase IV C subunit
ParE	Topoisomerase IV E subunit
pNO1	Plasmid NO1
rpm	Revolutions per minute
S. aureus	*Staphylococcus aureus*
SAR	Structure-activity relationship
sp.	Species
TF	Triplex formation
TFO1	Triplex forming oligonucleotide
Topo (IV)	Topoisomerase (IV)

Tris HCl	tris(hydroxymethyl)aminomethane
Tw	Twist number
vs.	versus
Wr	Writhe number

Aim of work

The aim of this thesis is *in vitro* evaluation of gyrase B inhibitors, which were synthesized at the Department of Medicinal Chemistry at the University of Ljubljana, Slovenia. Evaluation of IC_{50} (acquired by enzymatic assay) will describe efficacy (and selectivity) of tested compounds. ITC will characterize mechanisms of binding and thermodynamic aspects. Obtained results should review and set out an efficient direction of further synthesis of functional novel gyrase inhibitors.

As Theoretical background of the thesis, DNA structure, DNA topology and its parameters, DNA topoisomerases type I and II, mechanism and structure of Gyrase and Topo IV and known inhibitors on the market will be described.

Introduction and principle of applied methods, materials and instrumental equipment used during experiments and procedure protocols will be described in Experimental part.

1 Introduction

Although antibiotic active substances have been empirically used since ancient times, the first science-based discoveries were recorded in the late 19th century; the greatest success turned up in the 20th century with the discovery of penicillin by Alexander Fleming in 1929. A huge boom in usage of antibiotics came with the Second World War, since when it have saved thousands of lives. Since then, many other groups of substances have been discovered, many other molecules have been tested and described; whether they were natural antibiotics or chemically synthesized chemotherapeutics, acting by a different mechanism targeting different microorganisms, with different tolerance and efficiency. Today, many of these discoveries have irreplaceable role in the treatment of infections and are considered absolutely essential and necessary. With the high rate of use, sometimes even misuse (overuse) of antibiotics, however, the degree of resistance to these agents increases and complicates treatment of formerly easily manageable infections. This problem is becoming more significant and begins to threaten human health and lives. Therefore, modern science tries to fight against this phenomenon, whether searching for new ways of suppression of infectious agents and substances for this purpose, or revelation of specific mechanisms of antibiotic resistance and its prevention.

This paper deals with the first mentioned way. Since aminocoumarine antibiotics are not further used in clinical practice due to major side effects, new molecules are being synthesized and evaluated. This thesis determines the antibacterial activity of novel inhibitors of topoisomerases, enzymes essential for the function of bacterial cells. Specifically, gyrase or topo IV were described as very operative targets of inhibition and promise interesting results to the future. It is only the first step on a long journey, but hopefully this will help contribute to the introduction of new, more effective drugs and to improve the pharmacotherapy of infections.

2 Theoretical background

2.1 DNA structure

The structure of DNA is known since 1953 when Watson and Crick presented their model of double helix. DNA strands are formed by nucleotides – repeating units consisting of sugar component (2'-deoxyribose), phosphate and purine (adenine, guanine) or pyrimidine (cytosine, thymidine) bases, respectively. [1]

Primary structure of DNA – single strand – is created by a phosphodiester linkage binding 3'-hydroxyl group of one sugar component and 5'-hydroxyl group of the other. Bases are attached to 1'-position of 2'-deoxyribose. Secondary structure (double helix) is formed by two antiparallel strands – phospodiester binding in 3'-5' direction and 5'-3' direction, respectively. [1-3]

The most common form of the secondary structure of DNA molecule discovered in most of the cells is called B-form, or C2´-endo conformation. B-form is described as right-handed double helix with 10.5 base pairs (bp) for each turn of the helix; bases are perpendicular to the axis. However, two more conformations of double helix are also known – A-form and Z-form[1]. [1, 3]
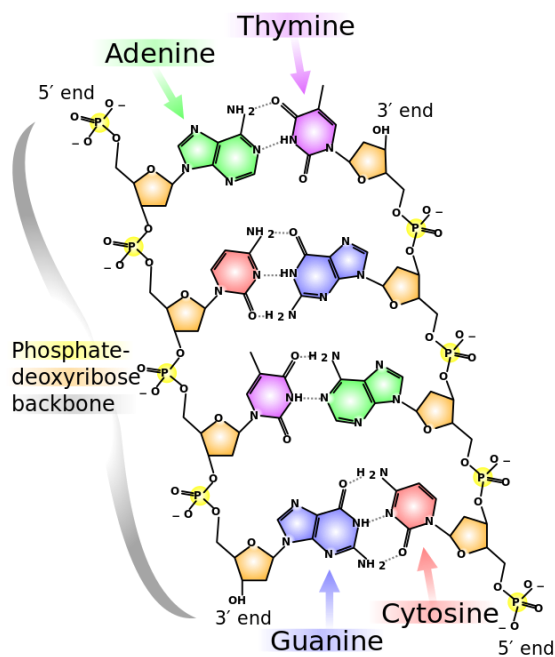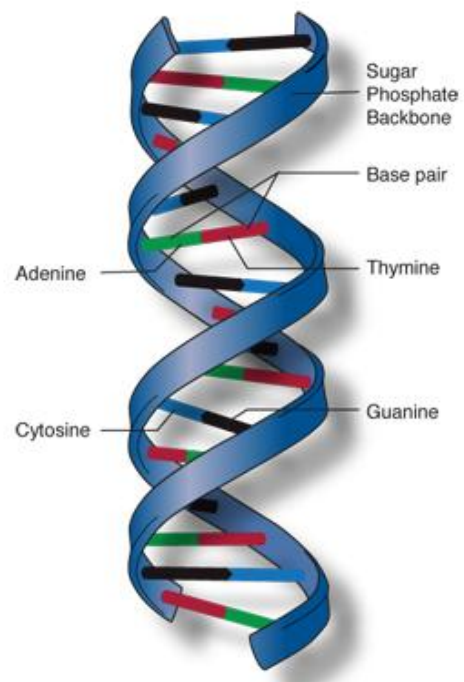

Figure 1: DNA primary structure. [4]

Figure 2: DNA secondary structure. [5]

---

[1] **A-form** is right-handed double helix with C3´-endo conformation, bases are not perpendicular to the axis and major groove is covered with phosphates and therefore hardly approachable for proteins.
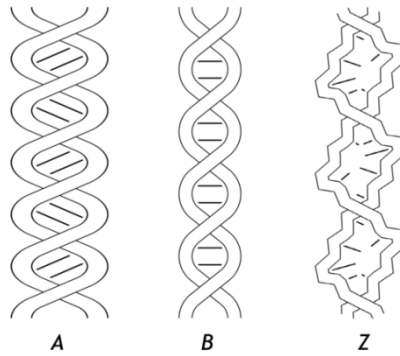**Z-form** is left-handed double helix with zig-zag conformation. [1]

Figure 3: Scheme of different forms of DNA molecule. [6]

2.1.1 Prokaryotic cells

Genetic information of the prokaryotic cell is stored in a single circular chromosome, called nucleoid. It consists of negatively supercoiled double-stranded DNA molecule. Prokaryotic cells do not contain defined nucleus (which would be bounded by a nuclear membrane), nucleoid is located in the central part of the cell, highly condensed (using supercoiling). In some cases, nucleoid is attached to an invaginated section of the cell membrane called a mesozome. [3] Most of the prokaryotic chromosome is formed by genes (coding units), there is minimum of "junk DNA". [7]

In the prokaryotic cell we also distinguish several types of plasmids - smaller circular dsDNA molecules which are autonomous and independent of the activity of the nucleoid. Inter alia, plasmids are responsible for resistance to antibiotics, and thus are frequent subjects of research of modern science. [1, 3]
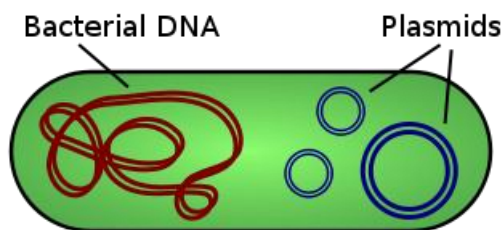
Figure 4: Scheme of prokaryotic cell. [8]

2.1.2 Eukaryotic cells

The eukaryotic cell contains the nucleus bounded by nuclear membrane to separate chromosomes from other organelles. Unlike prokaryotes, eukaryotic chromosomes contain a large number of introns, non-coding sequences. Since the linear length of eukaryotic DNA strain is enormous, it needs to be condensed into complex with protein, called chromatin. Nucleosome is basic unit of chromatin chain – 146 bp of double helix are turned around histone octamer in 1.6 left-handed turns. Basic units are repeating; this formation reminds "beads on a string", according to what is called. [1]

Histones are positively charged proteins which interact with negatively charged phosphate backbone of DNA double helix; protein H1 is attached to it where DNA starts and ends the turn around protein octamer (H2A, H2B, H3, H4). Nucleosomes are further wrapped into a solenoid (8-10 nucleosomes; 30 nm), and finally into the eukaryotic chromosome[2]. One chromosome corresponds with one DNA molecule. [1, 3] The process of condensation is schematically shown in Figure 6.

Beside nuclear DNA, we also distinguish a mitochondrial DNA (mtDNA) – circular double-stranded DNA molecules stored in mitochondria, semi autonomic organelles. [3]

Figure 5: Structure of the nucleosome. [9]

Figure 6: Scheme of condensation levels of DNA molecule. [10]

---

[2] Level of condensation differs according to the cell cycle phase. Heterochromatin and metaphase chromosomes are highly compacted, while interphase chromosomes are only slightly condensed into euchromatin. [3]
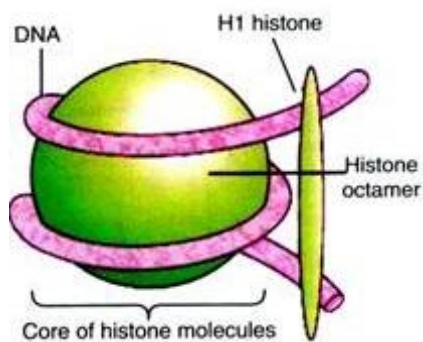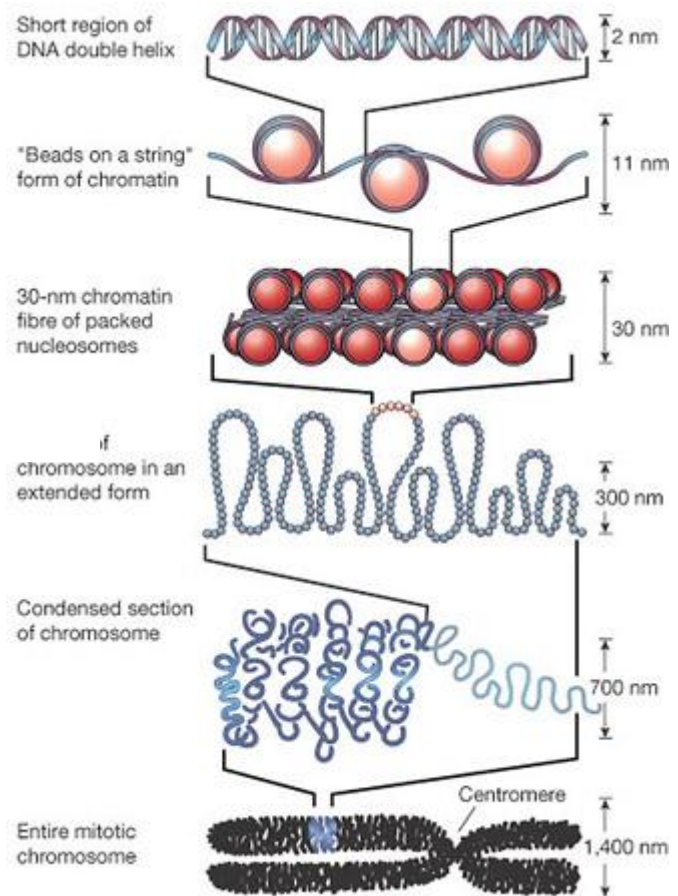
2.2 DNA topology

For a proper function, DNA double helix needs to be untangled. However, cccDNA (covalently closed circular DNA) structure does not contain free ends of strands, untangling is restricted and torsional stress is caused (DNA is topologically closed). The tension can be altered by supercoiling – helix is winding around itself. [7] This phenomenon appears during replication, when replication fork is created and strands are being separated, but also in the idle DNA molecule[3]. Supercoiling is an important mechanism of "packaging" DNA into space-efficient structures. [1, 7, 11]

DNA topology mathematically describes the geometry of DNA molecule, topological changes and alteration mechanisms. It introduces terms such as supercoiling and its quantitative expressions, described in sections 2.2.1 - 2.2.6. [7] Parameters of DNA topology are altered by strand-breaks introduced by DNA topoisomerases, as described in chapter 2.3.

2.2.1 Supercoiling

Supercoiling describes a shape of DNA molecule. There are two basic configurations of supercoiled DNA molecule – solenoidal and plectonemic, defined according to form of writhe (see 2.2.3). [12] First mentioned configuration occurs in eukaryotic cells, when chromatin fibre is wrapped around nucleosomes and creates solenoids, further condensed into the heterochromatin (see 2.1.2). [13] On the other hand, plectonemic or interwound configuration is typical for prokaryotic cells. [11] The configurations are easily convertible.

2.2.2 Linking number

Linking number (**Lk**) describes the topology of DNA molecule, it represents amount of tension. Linking number is defined as theoretical number describing how many times would one strand of a circular dsDNA have to pass over the other one leading to complete separation. [11, 12] It always has to be an integer; however, we determine positive and negative values. By the convention, linking number of right-handed double helix is positive. [1] Linking number is invariant; it cannot be changed by any deformation of DNA molecule, except of breaking the strands. [11]

Linking number of relaxed DNA molecule or plasmid (**Lk°**) is determined as length of DNA $N\ [bp]$ divided by a number of base pairs per turn, $h\ [bp]$ which is 10.5 bp in case of B-form DNA, as mentioned above[4].

$$Lk° = \frac{N}{h} = \frac{N}{10.5} \tag{1}$$

---

[3] It is often compared to telephone cord, or rubber tubing model. [7]
[4] Due to this calculation, Lk° value does not have to be an integer. It only serves as a reference point for level of supercoiling.

2.2.3   Twist and writhe

Twist number (Tw) "is a number of helical turns of one strand about the other". [12] When circular DNA is lying flat in the plain, the twist number equals to the linking number. [1] *Tw* for right-handed double helix is more than zero and conversely for left-handed helix, as shown in the Table 1.

Writhe number (Wr) is number of turns of the helix around itself, creating the superhelix. The range of values is opposite to the twist number.

Type of helix	Tw	Wr	Lk
Right-handed helix	> 0	< 0	> 0
Left-handed helix	< 0	> 0	< 0

Table 1: Range of values of twist or writhe number, according to the direction of rotation of the helix.

The sum of twist and writhe always gets the linking number, although Tw and Wr values do not have to be integers necessarily.

$$Lk = Tw + Wr \tag{2}$$

2.2.4   Linking difference

As Lk° is linking number of relaxed DNA molecule and Lk is linking number of supercoiled DNA molecule, a quantitative measure of supercoiling (in other words, an actual number of turns), is expressed by **linking difference (ΔLk)**. [11]

$$\Delta Lk = Lk - Lk° \tag{3}$$

Linking difference also corresponds with any changes of twist or writhe numbers: [1]

$$\Delta Lk = \Delta Tw + \Delta Wr \tag{4}$$

Most DNA molecules *in vivo* are negatively supercoiled; it means that the value of ΔLk is less than zero (negative), and therefore negatively supercoiled DNA is unwound by comparison with relaxed molecule. However, positive supercoiling is also possible and occurs when ΔLk is more than zero (positive), DNA is overwound. It was found in thermofilic microorganisms living in environment with extremely high temperature. Positive supercoiling and hence stored free energy prevents them from DNA denaturation. [12]

2.2.5 Specific linking difference

Another parameter – **specific linking difference (σ)**, sometimes called **superhelical density**, is useful for comparisons between DNA molecules with different size. It is more suitable than ΔLk because it does not consider an actual length of DNA molecule, but it estimates the number of supercoiles per helical turn[5]. [11]

$$\sigma = \frac{\Delta Lk}{Lk°} = \frac{h \cdot \Delta Lk}{N} \tag{5}$$

2.2.6 Knotting, catenation

Additional topological characteristic are knotting and catenation, respectively. Both conditions cannot be changed by any conformational alteration, only by breakage of the strands, so clearly action of topoisomerases is needed. Catenanes – covalently closed linked DNA molecules are often created at the end of replication process and their separation is essential for cell division.

Sporadically, knotting results from various processes, e.g. recombination. Again, covalent bonds can be only unknotted by DNA topoisomerases. Mechanism and types of the reactions carried out by particular types of topoisomerases are described in chapter 2.3. [11, 12]

2.2.7 Thermodynamics

However, supercoiling is energetically inconvenient process. Although it alters torsional tension, elastic deformations (twisting, bending) are being introduced and formed energy results as a free energy of supercoiled DNA molecule. Free energy can be defined as product of gas constant $R \; [J \cdot K^{-1} \cdot mol^{-1}]$, absolute temperature $T \; [K]$, length of DNA $N \; [bp]$ and squared specific linking number σ.

$$\Delta G = 10 \cdot RTN\sigma^2 \tag{6}$$

To alter energetic disfavor, minor supercoil relaxation is being performed. Hence, negatively supercoiled double helix tends to unwind, while positively supercoiled one tends to overwind. [1, 11]

---

[5] For example, specific linking difference of circular DNA from the living cells varies between 0.02 to 0.09, which indicates 2-9 supercoils per 100 helical turns. [11]
Also, specific linking difference of isolated bacterial plasmids or *E. coli* chromosome was -0.06, although their size is very different. [1]

2.3 DNA topoisomerases

DNA topoisomerases occurred in each examined cell type. These enzymes are responsible for conversions of different topological types of DNA – topoisomers[6]. First enzyme from this group was discovered in 1971 by James Wang. [14, 15] Today, we know many others. According to the mechanism of cleavage, they are divided into two groups – I and II. All types of topoisomerases can catalyze relaxation of negatively supercoiled DNA. However, other reactions are also possible and are unique for each type of topoisomerases. Some of them are shown in the Table 2.

Because of their function – release torsional stress caused by supercoiling (mechanism described in chapter 2.3.3), topoisomerases are essential for replication, transcription, recombination or chromosome condensation. [11]

Enzyme	Type	Source	Size (kDa) /structure	Special characteristic
Bacterial topo I (ω protein)	IA	Bacteria (e.g. *E. coli*)	97 monomer	Only negative supercoiling
Eucaryotic topoisomerase I	IB	Eukaryotes	91 monomer	Can relax both positive and negative supercoiling
Reverse gyrase	IA	Thermophilic Archaea (e.g. *Sulfolobus acidocaldarius*)	143 monomer	Can introduce *positive supercoils* into DNA (ATP-dependent)
DNA gyrase	IIA	Bacteria	97/90 A_2B_2	Can introduce *negative supercoils*
Topoisomerase IV	IIA	Bacteria	84/70 C_2E_2	Potent decatenase
Eucaryotic topoisomerase II	IIA	Eukaryotes	174 homodimer	
Topoisomerase VI	IIB	Archaea (e.g. *Sulfolobus shibatae*)	45/60 A_2B_2	

Table 2: Characterization of selected examples of topoisomerases: type, subunit size and composition, other characteristics. [1]

---

[6] Topoisomers are DNA molecules with the same length and sequence, but different topological parameter.

2.3.1 DNA topoisomerases I

Type I of DNA topoisomerases includes enzymes which break only one strand of DNA for relaxing the tension resulting supercoiling. Except Reverse gyrase[7], all other type I topoisomerases are ATP-independent. Except of *Methanopyrus kandleri* reverse gyrase, all type I topoisomerases are monomers. [16]

DNA topoisomerases I are divided into the subfamilies A and B (formerly designated as I-5' and I-3', respectively [15]); recently new type IC with only representative *Methanopyrus kandleri* Topo V was defined. [17, 18] Both IA and IB types alter twist number, although with different mechanism. After breaking one strand of double helix, IA topoisomerases pass the cleaved strand through the break and reconnect it (only one turn is released), while IB topoisomerases rotate the other side (unbroken strand) by swivel mechanism by one or more turns. [7, 15]

Characteristic factors for IA type:

- enzyme binds to 5' phosphate end of exposed single-stranded segment of DNA;
- DNA relaxation requires Mg(II);
- only negative supercoiling can be relaxed;
- relaxation is partial;
- by relaxation, linking number is changed in steps of one;
- IA enzymes also catalyze knotting, unknotting, interlinking (single-strand DNA) and catenation and decatenation (double-strand DNA with gaps or nicks).

Characteristic factors for IB type:

- can relax both positive and negative supercoiling;
- covalent bond to 3´phosphate end of double-stranded DNA;
- relaxation in both cases goes to completion;
- DNA relaxation does not require Mg(II);
- Lk is changed by any integer [14, 16].

2.3.2 DNA topoisomerases II

The other type of topoisomerases – type II – includes enzymes which break both strands of DNA; after that, one strand is passed through another (writhe number is altered, Lk is changed in steps of 2) [7]. Phosphodiester bond between tyrosine and DNA frame is attached to 5´ phosphate end (in both subfamilies, A and B). Also, Mg(II) is required and reactions are ATP-dependent (energy from ATP hydrolysis is needed, ADP is formed). [16]

---

[7] With energy of ATP hydrolysis, reverse gyrase can introduce positive supercoiling in thermofilic bacteria, similarly as DNA gyrase can introduce negative supercoiling, although they are not homologues and even belong to different families.

Mechanism of action and structure of IIA and IIB topoisomerases are similar; the main difference is in the structure of DNA-enzyme complex (4 bp or 2 bp overhangs, respectively). [14]

The reactions carried out by DNA topoisomerases II are shown in Figure 7. The reactions can run in both directions[8]. Tending to specific type of reaction is one of the tools to distinguish types of DNA topoisomerases II.
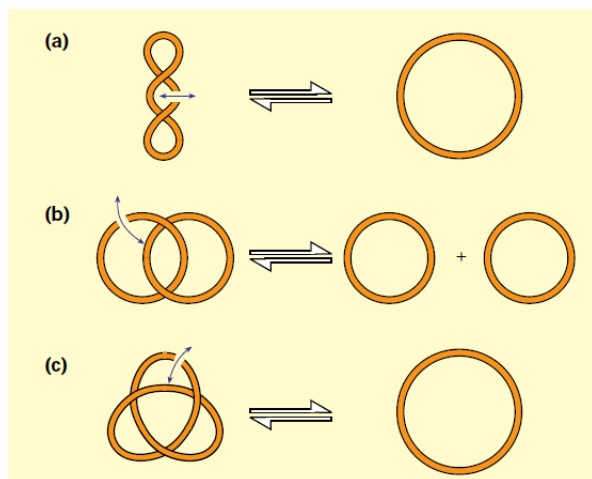

Figure 7: Scheme of possible reactions performed by topoisomerases.
(a) supercoiling ↔ relaxation
(b) catenation ↔ decatenation
(c) knotting ↔ unknotting [19]

Basic characteristic of all types of topoisomerases is summarized in the Table 3.

Characteristic	*IA*	*IB*	*IIA*	*IIB*
Cleavage	Single-strand		Double-strand	
DNA-enzyme binding	5´ phosphate end	3´phosphate end	5' phosphate end	
ATP-dependent	NO[a)]	NO	YES	
Mg(II) requirement	YES	NO	YES	
Alteration	twist		writhe	
Lk change	1	Z	2	
Supercoiling relaxation	Negative only	Positive and negative	Positive and negative	

Table 3: Basic characteristic of all types of topoisomerases.
a) except of reverse gyrase

According to the Table 2, DNA gyrase and topoisomerase IV (topo IV hereinafter) belong to IIA subfamily of DNA topoisomerases. Since the experimental part of this thesis is focused on these two enzymes, the following chapters are devoted to them.

---

[8] Type I topoisomerases can also perform those reactions, although reactions (b) and (c) from Figure 7 require nick in double-stranded DNA molecule.

2.3.3 Structure and mechanism

Both DNA gyrase and topo IV have two domains – ATPase and DNA binding/cleavage domain located on two different polypeptide chains, in case of bacterial topoisomerases[9]. DNA gyrase and topo IV are presented as heterotetramers. The subunits of both enzymes are structurally and functionally similar and some of topo IV functions can even be compensated by gyrase. [14, 20]

2.3.3.1 DNA gyrase

DNA gyrase consists of two subunits A (97 kDa) and B (90 kDa). Altogether, they form tetramer A_2B_2. GyrA subunit is responsible for binding and breaking DNA strand, while GyrB subunit performs ATPase activity. Proteins are coded by *gyrA* and *gyrB* gene, respectively, which were defined as genes responsible for resistance to inhibitors (nalidixic acid or coumermycin A).

DNA gyrase is the only topoisomerase which can introduce negative supercoiling by conversion of free energy from ATP hydrolysis. In addition, gyrase can also relax both negative and positive supercoiling and catenate/decatenate or knot/unknot DNA molecules. [21, 22]

The general mechanism of gyrase action (as well as mechanism of all type II topoisomerases) is described as two-gate model. Both strands of DNA part called G-segment (G as *gate*) are cleaved and attached by 5' phosphate to active-site tyrosine of GyrA (N-terminal domain). The conformation of enzyme now contains open protein gate formed by ATP-operated clamps, so T-segment of DNA (T as *transported*) can pass through G-segment. ATP binding on GyrB results in closing of the clamps (N-terminal domain) and opens another protein gate on the other side of the enzyme, so T-segment can exit. ATP hydrolysis changes the conformation of first protein gate to open-state again. This process can be carried out on intramolecular or intermolecular level. When G-segment and T-segment are on the same molecule, relaxation or unknotting will happen. Decatenation occurs when segments are on different molecules. [15, 19, 20, 23]

Unique gyrase-related introducing of negative supercoils is produced by wrapping DNA (about 130 bp, including G-segment) around C-terminal domain of GyrA and delivering T-segment to the ATP-operated clamp in particular orientation. [19, 21]

2.3.3.2 Topoisomerase IV

Topo IV has tetrameric structure described as C_2E_2. ParC (84 kDa) and ParE (70 kDa) corresponds with GyrA and GyrB, respectively. Topo IV is not able to introduce negative supercoils, but otherwise mechanism of reactions is the same as is for gyrase. [14] However, topo IV prefers decatenation to relaxation. [19, 20]

---

[9] Domains of eukaryotic topoisomerases are placed on one polypeptide chain.
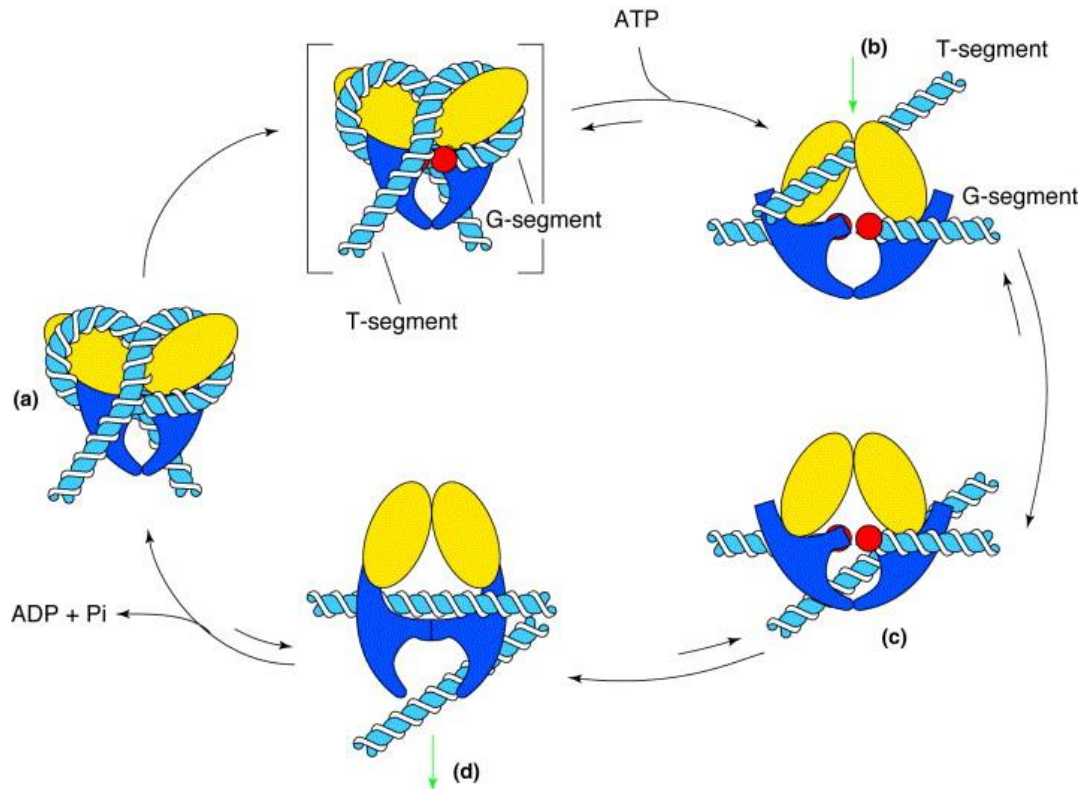
Figure 8: Scheme of gyrase mechanism of action.

Gyrase consists of two GyrA subunits (blue) and two GyrB subunits (yellow).

(a) 130 bp DNA segment is wrapped around the enzyme. G-segment is cleaved and attached to 5'-phosphate of GyrA.

(b) ATP binds to the enzyme and induces conformational change of GyrB subunits. It also holds cleaved G-segment apart to allow transition of T-segment.

(c) T-segment passes through the enzyme and G-segment.

(d) G-segment is linked together again, another protein gate on the other side is created and T-segment can exit the complex. ATP hydrolysis and allow enzyme to regenerate to the original state (a). [24]

2.4 Inhibitors of topoisomerases used in clinical practice

DNA topoisomerases have an irreplaceable role in the cell growth; therefore they are promising potential targets of cytotoxic drugs. Inhibitors of prokaryotic topoisomerases are used as antibacterial agents, while inhibitors of eukaryotic topoisomerases have important role as anticancer drugs. [1]

2.4.1 Antibiotics

There are two main groups of drugs with antibiotic effect – quinolones and aminocoumarins. They both inhibit DNA gyrase and topoisomerase IV, although with different mechanism.

2.4.1.1 Quinolones

Quinolones are synthetic derivatives of 4-oxo-1,4-dihydroquinolone frame. [20] The first molecule from quinolone family – **nalidixic acid** – was placed on the market in 1960's. [25] Since then, many other derivatives were discovered and today, they form already 4th generation[10]. [26]
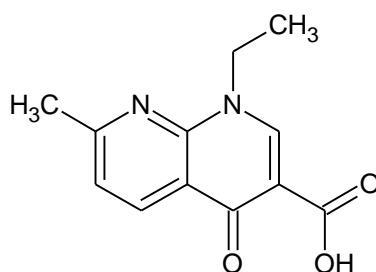
Scheme 1: Structure of nalidixic acid.

Mechanism consists in inhibition of type II topoisomerases (gyrase and topo IV). Drug molecule binds to GyrA-DNA complex and changes protein conformation. This action, called also stabilization of cleavable-complex, leads to change of ATPase activity, prevents DNA molecule from reuniting broken strands and induces fatal disruption. [1, 27, 28]

Fluoroquinolones are broad-spectrum antibiotics with bactericidal effect used mainly for treating infections of respiratory and urinary system, as well as bones, skin and soft tissues infections. Although they show several side effects, such as nausea, headache, vomiting, chondrotoxicity or phototoxicity, in general they are well tolerated. Admittedly, fluoroquinolones are teratogenic. [29] Examples of clinically used quinolones are shown in the Table 4.

However, clinically significant resistance has appeared. The mutations in DNA gyrase and topo IV cause weakening of interaction between quinolones and enzymes. New molecules are being tested to expand the range of molecules for efficient treatment. [25]

---

[10] Fluorine has been introduced into the molecule since 2nd generation. So-called fluoroquinolones have advanced physic-chemical properties and broader spectrum of effect. [29]

Class	API	Agens
1st generation	nalidixic acid oxolinic acid	Gram-negative bacteria
2nd generation	ciprofloxacin ofloxacin norfloxacin pefloxacin profloxacin	Gram-negative bacteria Gram-positive bacteria *Pseudomonas aeruginosa* *Chlamydia* sp. *Legionella* sp. anaerobic bacteria
3rd generation	levofloxacin gatifloxacin sparfloxacin	Gram-positive bacteria anaerobic bacteria
4th generation	trovafloxacin alatrofloxacin moxifloxacin	Gram-positive bacteria anaerobic bacteria

Table 4: Quinolones used in clinical practice and their spectrum of action.
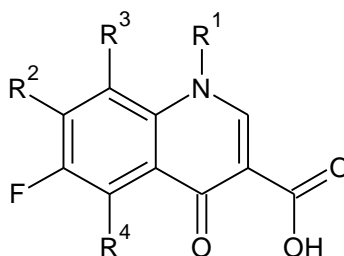
Scheme 2: Basic structure of fluoroquinolones.

Compound	*R¹*	*R²*	*R³*	*R⁴*
norfloxacin	-CH₂CH₃	piperazinyl	H	H
ciprofloxacin	cyclopropyl	piperazinyl	H	H
sparfloxacin	cyclopropyl	3,5-dimethylpiperazinyl	F	NH₂
gatifloxacin	cyclopropyl	3-methylpiperazinyl	OCH₃	H
moxifloxacin	cyclopropyl	octahydropyrrolo[3,4-b]pyridinyl	OCH₃	H

Table 5: Substituents of selected fluoroquinolones, attached to basic structure pictured on Scheme 2.
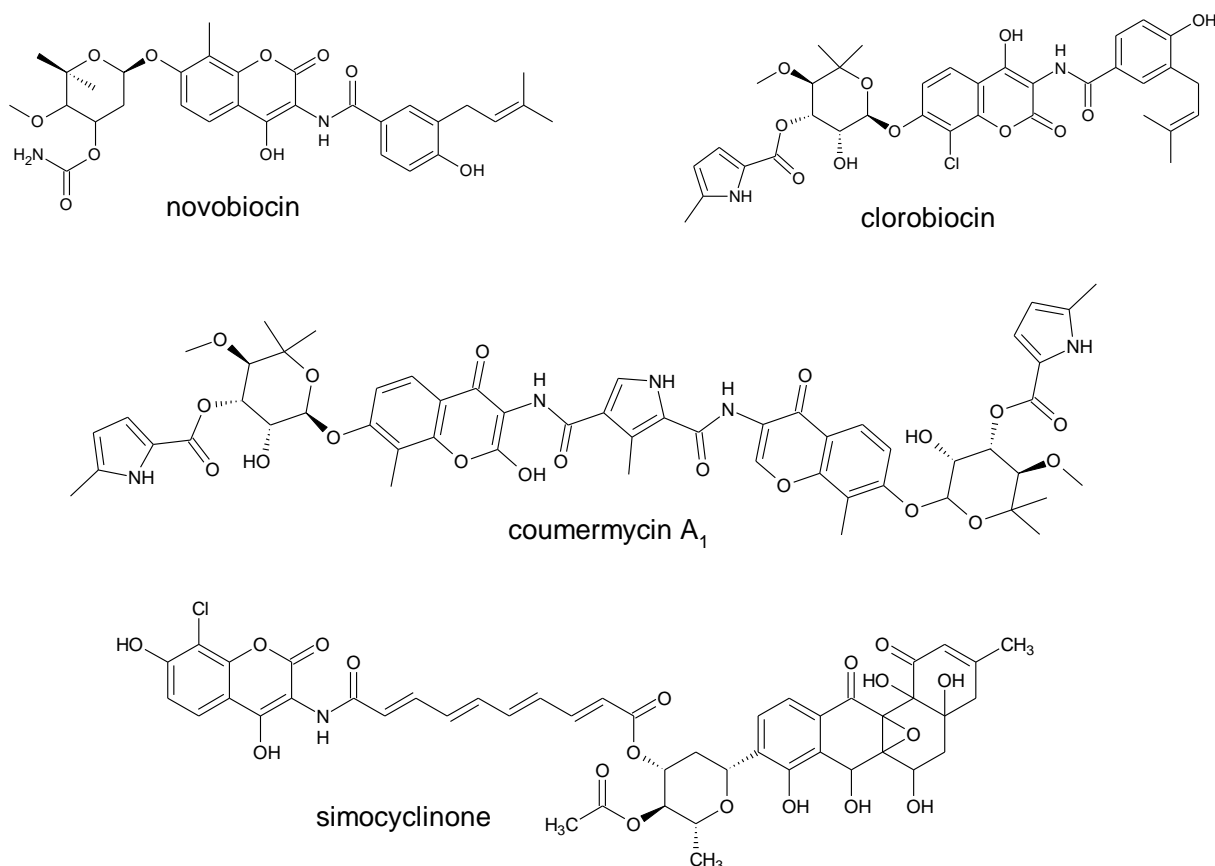
2.4.1.2 Aminocoumarins

The class of aminocoumarin antibiotics is derived from product of *Streptomyces* sp. Aminocoumarins have been known since 1950's; first representative **novobiocin** was licensed for clinical use in 1960's.

Mechanism of action is inhibition of ATPase reaction. Aminocoumarins act as competitive inhibitors[11]. They bind to ATP-binding site of GyrB subunit instead of ATP molecule and stop ATP hydrolysis, essential for the next steps of gyrase activity.

Clinical use of aminocoumarins has been limited because of low solubility (thus poor bacterial cell permeation), frequent side effects (eukaryotic toxicity) and increasing resistance. However, new molecules of aminocoumarin class with less side effects and better physico-chemical properties are being synthesized. [22, 30]

The discovery of new aminocoumarin representative promises an interesting direction of future researches. **Simocyclinone D8** is also product of *Streptomyces* sp., but deoxysugar moiety is missed out from the structure. Inhibitor therefore cannot bind to GyrB as the other aminocoumarins, but it binds to two sites of GyrA (different from quinolone-site) and prevents enzyme from binding to DNA strand. It constitutes an entirely new mechanism of topoisomerases inhibition. [30]

novobiocin

clorobiocin

coumermycin A₁

simocyclinone

Scheme 3: Structures of aminocoumarins.

---

[11] Surprisingly, aminocoumarins and ATP molecule are not very structurally similar, as we would expect. However, binding mechanism was proved by X-ray crystallography. [20]

2.4.2 Anticancer drugs

Inhibitors of topoisomerases are also used for cancer treatment. Inhibitors act on eukaryotic topoisomerases and induced replication-dysfunction results in stopping increased cell proliferation, typical for tumors. Cytostatics from this class are of plant origin or derivatives. They inhibit enzymes from both families – topoisomerases I and II. [1, 28]

2.4.2.1 Camptothecin and its derivatives

Camptothecin[12] and its derivatives are targeted to human topoisomerase I. Mechanism of action is similar to quinolones (described in chapter 2.4.1.1) – drug molecule stabilizes enzyme-DNA complex; broken DNA cannot be replicated and it leads to the apoptosis. Nowadays, derivatives such as **topotecan** and **irinotecan** are used in clinical practice due to their higher efficiency and lower toxicity. Topotecan is used for ovarian carcinoma treatment. Irinotecan is the prodrug used for colorectal, bronchogenous, ovarian and cervix carcinoma treatment. [28, 31]
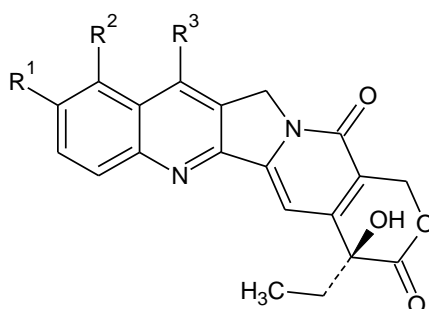
Scheme 4: Basic structure of camptothecin derivatives.

Compound	R¹	R²	R³
camptothecin	H	H	H
topotecan	OH	H_2C-N with CH_3, CH_3	H
irinotecan	(piperidine-piperidine carbamate structure)	H	C_2H_5

Table 6: Substituents of camptothecin derivatives attached to basic structure pictured on Scheme 4.

---

[12] Camptothecin was isolated from *Camptotheca acuminata*, also known as Happy Tree and used in Chinese traditional medicine for cancer treatment.

2.4.2.2 Epipodophyllotoxin and its derivatives

Podophyllotoxin is mitotic inhibitor used topically for treatment of viral papillomas. It is one of the active substances contained in podophyllin[13]. Glycosides derived from 4'-demethyl-9-epipodophyllotoxin – **etoposide**, **teniposide** - are inhibitors of toposiomerase II. They stabilize covalent enzyme-DNA complex, and in addition, they intercalate into DNA. These drugs have quite broad spectrum of indications – acute leukemia, malign lymphomas, testicular tumors and bronchogenous carcinoma. [28, 31]
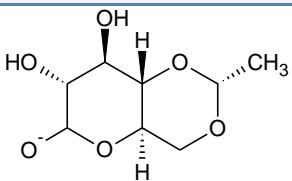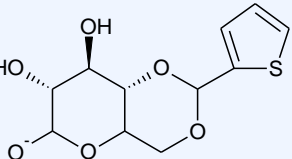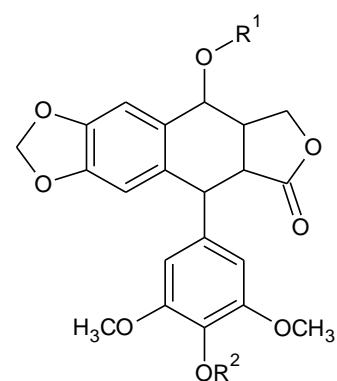
Compound	R^1	R^2
podophyllotoxin	H	CH_3^-
etoposide		H
teniposide		H

Table 7: Substituents of podophyllotoxin derivatives possibly attached to basic structure pictured on Scheme 5.

Scheme 5: Basic structure of podophyllotoxin derivatives.

2.4.2.3 Intercalating agents

These molecules have planar structure, hence easily intercalate between bases in DNA molecule, using the hydrogen bond. It leads to inhibition of RNA synthesis and DNA replication (they mostly operate during S and G_2 phase of cell cycle). Common side-effect of intercalating agents is cardiotoxicity caused by free oxygen radicals. [31]

First representative of **anthracycline antibiotics** is **doxorubicin** isolated from *Streptomyces peucetius.* Beside intercalation mechanism, doxorubicin interacts with cell membrane; therefore both structure and function of the cell are damaged. It is used for hematologic malignancies, breast cancer, ovarian, endometrial or stomach carcinoma treatment. Its analogues – **idarubucin, epirubicin** – have lower cardiotoxicity. [28, 31]

Anthraquinone derivatives represented by **mitoxanthron** are similar to anthracycline antibiotics. In this case, free radicals are not created. It is used for e.g. breast cancer, acute leukemia or lymphomas treatment.

---

[13] Podophyllin is resinous extract from the rhizome of *Podophyllum peltatum* or *Podophyllum emodi.*

Acridine derivative **amsacrine** is used for acute myeloblastic leukemia (AML) and acute lymphoblastic leukemia (ALL) treatment. [31]
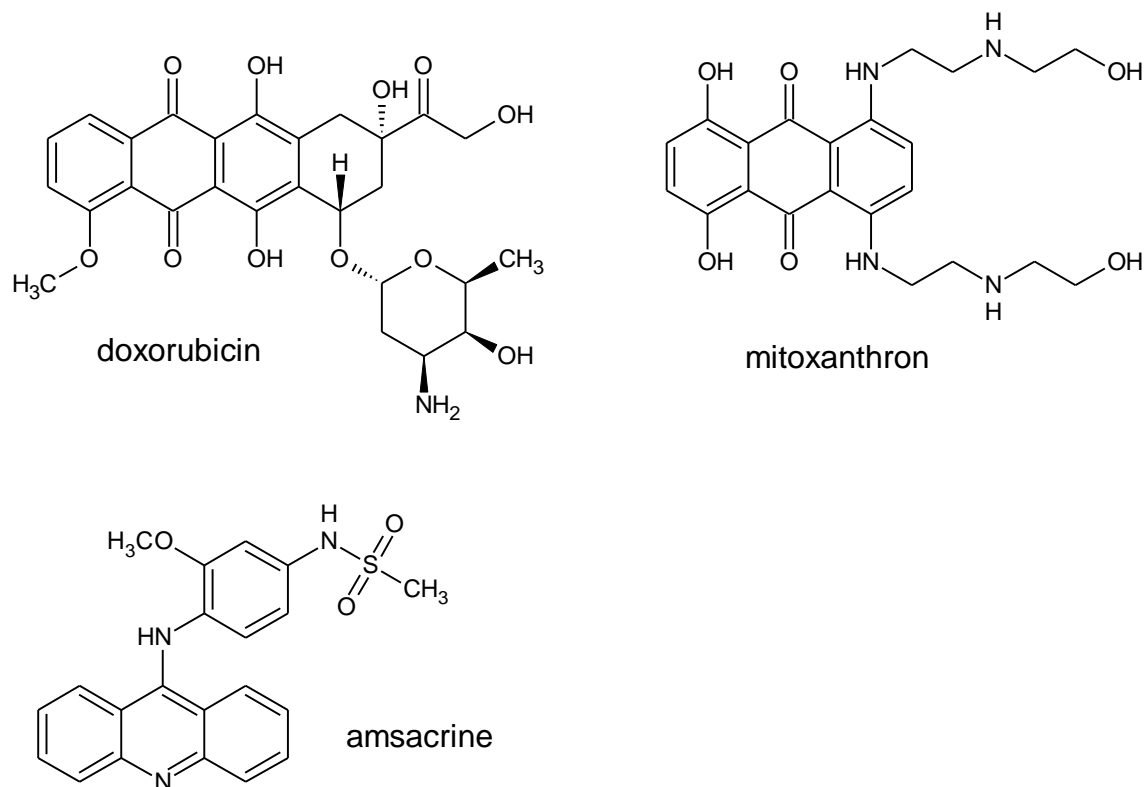
Scheme 6: Structures of selected intercalating agents.

Class	Representatives	Target	Indication
Camptothecin derivatives	topotecan irinotecan	topo I	ovarian, colorectal, bronchogenous, cervix carcinoma
Podophyllotoxin derivatives	etoposide teniposide	topo II	acute leukemia, lymphomas, testicular tumors
Acridin derivatives	amsacrine	topo II	AML ALL
Anthracycline antibiotics	doxorubicin daunorubicin epirubicin idarubicin mitoxanthron	topo II	hematooncology, breast cancer, ovarian, endometrial, stomach carcinoma lymphomas

Table 8: Summarization of used anticancer drugs, their targets and indication.

3 Experimental part

3.1 Supercoiling/Relaxation Enzymatic Assay

3.1.1 Principle of the method

High-throughput mictrotitre plate assay is based on ability of immobilized oligonucleotide to bind supercoiled DNA and form intermolecular triplex formation[14] (negatively supercoiled plasmid has higher affinity then relaxed plasmid).

Oligonucleotide TFO1 is bound to the wall of streptavidin-coated microtitre plate, thus immobilized. In case of

   a) supercoiling assay for DNA gyrase: relaxed plasmid pNO1 is added and supercoiled by gyrase (with Assay Supercoiling Buffer);
   b) relaxation assay for topo IV: supercoiled plasmid pNO1 is added and relaxed by topo IV (with Assay Relaxation Buffer).

The quantity of supercoiled plasmid in reaction volume is dependent on enzyme catalytic activity, hence efficiency of used inhibitor. Reaction is stopped by adding TF Buffer and lowering pH, relaxed (unbound) plasmid is washed off. Bound complex is then marked with fluorescent SYBRGold® staining and fluorescence is measured. The more probe-marked supercoiled plasmid is bound to oligonucleotide, the higher fluorescent signal we get, therefore

   a) greater activity of gyrase (lower inhibitor efficiency) leads to higher fluorescence – darker color resolution;
   b) greater activity of topo IV (lower inhibition) results in lower fluorescence – lighter color resolution.

As reference control, pNO1 without enzyme and novobiocin in two different concentrations were used. Concentration of DMSO, which was used as solvent of inhibitors, could not be higher than 3%. Enzymatic assay can be used for activity screening as well as for IC_{50} [μM] determination, if wide range of inhibitor concentration is prepared. [32-35]

---

[14] Triplex formation is alternative structure to double helix.

3.1.2   Materials and instruments

Except SybrGold® stain (Invitrogen), all the material was supplied by Inspiralis as Microplate Assay Kit which contains:

- Enzyme
- Plasmid pNO1
- TFO1 oligonucleotide
- Wash Buffer (supplied as 20× stock)
- TF Buffer (triplex formation, supplied as 20× stock)
- Assay Buffer (supplied as 5× stock)
- Enzyme Dilution Buffer
- T10 Buffer (supplied as 20× stock)
- 96-well streptavidin-coated black-walled plate (Thermo Scientific)

3.1.2.1   Enzymes

Four different enzymes were used for assay performing:

- *E. coli* gyrase (5 U/μl)
- *E. coli* topoisomerase IV (10 U/μl)
- *S. aureus* gyrase (10 U/μl)
- *S. aureus* topoisomerase IV (10 U/μl)

The enzymes are supplied as heterotetramers as a part of Assay Kit and must be stored at -80 °C. During assay performing, they should be kept on ice. Concentration of enzymes is expressed in [U/μl] in Dilution Buffer.

3.1.2.2   DNA substrate

DNA substrate was represented by pNO1 plasmid (relaxed or supercoiled pBR322, respectively, for gyrase or topo IV) in concentration of 1 mg/ml, and TFO1 oligonucleotide supplied at 10 μM.

3.1.2.3   Buffers

Concentrated buffers must be stored between -20 °C and -80 °C and must be diluted prior to use with ultra-pure water (DNase-free, autoclaved) according to the protocol described in chapter 3.1.3.

Buffer composition and concentration of components may vary depending on the type of kit, as shown in Table 9.

All the material was treated according to information provided by the manufacturer. [36]

	E. coli Gyrase Microplate Assay Kit	*S. aureus* Gyrase Microplate Assay Kit	*E. coli* Topo IV Microplate Assay Kit	*S. aureus* Topo IV Microplate Assay Kit
Wash Buffer	20 mM Tris.HCl (pH 7.6) 137 mM NaCl 0.01% (w/v) BSA 0.05% (v/v) Tween 20	20 mM Tris.HCl (pH 7.6) 137 mM NaCl 0.01% (w/v) BSA 0.05% (v/v) Tween 20	20 mM Tris.HCl (pH 7.6) 137 mM NaCl 0.01% (w/v) BSA 0.05% (v/v) Tween 20	20 mM Tris.HCl (pH 7.6) 137 mM NaCl 0.01% (w/v) BSA 0.05% (v/v) Tween 20
Assay Buffer	35 mM Tris.HCl (pH 7.5) 24 mM KCl 4 mM $MgCl_2$ 2 mM DTT 1.8 mM spermidine 1 mM ATP 6.5% (w/v) glycerol 0.1 mg/ml albumin	35 mM HEPES.KOH (pH 7.6) 10 mM magnesium acetate 10 mM DTT 2 mM ATP 500 mM potassium glutamate 0.05 mg/ml albumin	40 mM HEPES.KOH (pH 7.6) 100 mM potassium glutamate 10 mM magnesium acetate 10 mM DTT 1 mM ATP 50 µg/ml albumin	50 mM Tris.HCl (pH 7.5) 5 mM $MgCl_2$ 5 mM DTT 1.5 mM ATP 350 mM potassium glutamate 0.05 mg/ml albumin
Dilution Buffer	50 mM Tris.HCl (pH 7.5) 100 mM KCl 2 mM DDT 1 mM EDTA 50% (w/v) glycerol	50 mM Tris.HCl (pH 7.5) 1 mM DDT 1 mM EDTA 40% (w/v) glycerol	40 mM HEPES.KOH (pH 7.6) 100 mM potassium glutamate 1 mM DDT 1 mM EDTA 40% (v/v) glycerol	50 mM Tris.HCl (pH 7.5) 1 mM DDT 1 mM EDTA 40% (v/v) glycerol
TF Buffer	50 mM sodium acetate (pH 5.0) 50 mM NaCl 50 mM $MgCl_2$	50 mM sodium acetate (pH 5.0) 50 mM NaCl 50 mM $MgCl_2$	50 mM sodium acetate (pH 5.0) 50 mM NaCl 50 mM $MgCl_2$	50 mM sodium acetate (pH 5.0) 50 mM NaCl 50 mM $MgCl_2$
T10 Buffer	10 mM Tris.HCl (pH 8) 1 mM EDTA	10 mM Tris.HCl (pH 8) 1 mM EDTA	10 mM Tris.HCl (pH 8) 1 mM EDTA	10 mM Tris.HCl (pH 8) 1 mM EDTA

Table 9: Buffer composition in relevant kits.

3.1.2.4   DNA staining and equipment

Used 96-well streptavidin-coated black-walled plates were part of supplied kit. They must be stored covered in 4 °C.

SybrGold® stain (Invitrogen) was not part of the kit. It was stored in concentrated form in -18 °C and diluted with T10 buffer according to the protocol described in chapter 3.2.3.

Fluorescence measurements were carried out using BioTek® Synergy HT and evaluated by Gen5 Data Analysis software. IC_{50} values were determined by GraphPad.

3.1.3 Procedure

While performing microtitre plate assay, we had been following this protocol: [33, 36]

1. PLATE REHYDRATION
   a. Prepare Wash Buffer by diluting 7 ml of buffer with 133 ml of ultra-pure water.
   b. Rehydrate the wells three times with 200 µl of Wash Buffer.
   c. Remove all possible residues of buffer by aspirating.

2. IMMOBILIZATION OF THE NUCLEOTIDE
   a. Prepare TFO1 by diluting 725 µl of oligonucleotide with 13.775 ml of Wash buffer.
   b. Add 100 µl of TFO1 into each well.
   c. Allow immobilization process by incubating for 5 minutes at room temperature.
   d. Wash off excess oligonucleotide from the wells with 3×200 µl of Wash Buffer and remove all the liquid by aspirating.

✓ When working with *S. aureus* enzymes, wash the wells again with 200 µl of ultra-pure water and remove all the liquid after step 2.

3. INCUBATION OF THE ENZYME WITH THE SUBSTRATE
   a. Prepare the mixture of 760 µl of Assay Buffer, 2185 µl of ultra-pure water and 95 µl of pNO1.
   b. Add 24 µl of the mixture into each well.
   c. Prepare the enzyme by diluting:
       i. 40 µl of gyrase with 360 µl of Dilution Buffer
       ii. 20 µl of topo IV with 380 µl of Dilution Buffer
   d. Aliquot 3 µl of testing inhibitor and 3 µl of enzyme and let the reaction run while incubating at 37 °C for 30 minutes (in total reaction volume of 30 µl).

4. IMPLEMENTATION OF TRIPLEX FORMATION
   a. Prepare TF Buffer by diluting 5 ml of buffer with 95 ml of ultra-pure water.
   b. Add 100 µl of TF Buffer into the wells and incubate for 30 minutes at room temperature to allow triplex formation.
   c. After incubating, wash off unbound relaxed plasmid with 3×200 µl of TF Buffer and remove all the remained liquid by aspirating.

5. STAINING
   a. Prepare T10 Buffer by diluting 1.1 ml of buffer with 20.9 ml of ultra-pure water.
   b. Mix T10 Buffer with 2.2 µl of SybrGold®.
   c. Add 200 µl of the mixture into each well and let it proceed for 15 minutes at room temperature in the dark.

6. MEASURING
   a. BioTek® Synergy HT was used for fluorescence reading (Ex: 495 nm; Em: 537 nm).

3.2 ITC

3.2.1 Principle of the method

Isothermal titration calorimetry helps to determine thermodynamic parameters of biomolecular binding and interactions. ITC is based on precise measurement of released heat rate obtained during protein-ligand exothermic reaction[15]. The constant heat difference between reference and sample cell must be kept, or in other words, temperature in both cells must be equal. Actually, power used for the compensation of this difference is being measured [μJ/s]. [37]

Ligand (tested inhibitor) is being injected into sample cell with enzyme (*E. coli* GyrB); enzyme-ligand complex is created and the reaction heat is released. Then, feedback system starts to work and reaches the equilibrium. This phenomenon is recorded as a peak of certain height. One injection corresponds with one peak. When the system is saturated, we can still observe the peaks illustrating background heat. The area under the peaks is then integrated and fitted into independent binding model (blank is also considered, using base line as reference value) to determine affinity (K), enthalpy (ΔH) and stoichiometry (n). For calculations, relationship

$$\Delta G = -RT ln K_a = \Delta H - T\Delta S \tag{7}$$

is used, where $R\,[J \cdot K^{-1} \cdot mol^{-1}]$ is gas constant, $T\,[K]$ is absolute temperature, $K_a\,[M^{-1}]$ is binding affinity, $\Delta H\,[kJ/mol]$ is enthalpy and $\Delta S\,[kJ/mol]$ is entropy.

For proper determination, a "practical window" c was considered. K_a is binding affinity and $[M]_T$ is protein concentration. Concentration of ligand should be maximally 10× bigger than $[M]_T$.

$$10 < c = K_a \cdot [M]_T < 1000 \tag{8}$$

Binding affinity can be also described as inverse of dissociation constant K_d, which correlates with IC$_{50}$ value. [37-40]

$$K_a = \frac{1}{K_d} \tag{9}$$

---

[15] In our case, exothermic reaction was carried out. Naturally, endothermic reaction can proceed as well; then amount of absorbed heat is being measured.

3.2.2 Materials and instruments

3.2.2.1 Enzyme

E. coli GyrB domain of size 24 kDa and of stock concentration 2 mg/ml was used in the experiment. Enzyme was dialyzed and diluted with buffer pH 7.5 (20 mM Tris, 1 mM EDTA), aliquoted and stored at -80 °C.

3.2.2.2 Ligand

Prior to use, tested inhibitors were diluted with the same dialysis buffer as enzyme and with DMSO, if needed. In that case, the same amount of DMSO was added into enzyme solution. Since DMSO enhances enzyme inhibition, its final concentration in the sample could not exceed 3%.

3.2.2.3 Equipment

Measuring was performed using Nano ITC Standard Volume (TA Instruments). Data were obtained using ITCRun and analyzed by NanoAnalyse software.

3.2.3 Procedure

Both ligand and enzyme were degassed before measurement. Ligand in 10-15 µl aliquots was automatically injected 10 -16 times from microsyringe (250 µl) into sample cell (1.0 ml) with enzyme solution. Injection interval was 300 s. Specially adapted microsyringe simultaneously served as stirrer with constant speed 250 rpm. Measurement was carried out at 25 °C. The reference cell contained ultra-pure degassed water.

4 Results

4.1 Enzymatic assay

Tested compounds were synthesized at the Department of Medicinal Chemistry, Faculty of Pharmacy at the University of Ljubljana. Novel compounds with gyrase-inhibition (topo IV-inhibition) potential focused on ATP binding site of GyrB subunit were used.

Several series with different chemical composition were prepared and tested, but only some of them were tested for the purposes of this thesis. However, the base of the structure – **halogeno-1*H*-pyrrol-2-carboxamide** moiety appears in all compounds listed here.

Table 10 contains calculated IC_{50} values[16] of inhibitors from different series, but with activity against all types of used enzymes, ergo *E. coli* gyrase/topo IV and *S. aureus* gyrase/topo IV. Generally, the best results are found in *E. coli* gyrase (it is also most explored enzyme from this group).

Cmpd	*Structure*	*MW* [g/mol]	$IC_{50} [\mu M]$ *E. coli* *Gyrase*	$IC_{50} [\mu M]$ *S. aureus* *Gyrase*	$IC_{50} [\mu M]$ *E. coli* *Topo IV*	$IC_{50} [\mu M]$ *S. aureus* *Topo IV*
THT-19		431.29	0.29	10	210	130
KSK-25		431.29	0.39	320	300	290
KMG-9		488.11	0.053	360	13	10
KMG-11		502.14	0.11	4.7	40	14
KMG-15		399.20	0.087	0.35	1.8	1.7
KMG-17		413.23	0.12	8.5	5.2	3.1
KMG-31		516.16	0.12	*inactive*	*inactive*	*inactive*
KMG-32		516.16	0.24	*inactive*	-	*inactive*
KMG-33		527.91	0.87	*inactive*	*inactive*	*inactive*

---

[16] Half maximal inhibitory concentration specifies the concentration needed for 50% inhibition.

Cmpd	Structure	MW [g/mol]	IC$_{50}$ [µM] E. coli Gyrase	IC$_{50}$ [µM] S. aureus Gyrase	IC$_{50}$ [µM] E. coli Topo IV	IC$_{50}$ [µM] S. aureus Topo IV
TCF-3b		455.33	0.70	47	230	35
TCF-4b		441.30	0.72	7.3	150	5.2
TCF-4a		520.20	0.020	12	inactive	inactive
TMK-16		475.74	0.016	0.61	-	6.6
TNH-10		417.26	0.025	0.43	210	6.2
TJL-6		396.85	0.12	2.0	inactive	-
TJL-19		431.29	0.022	0.56	-	-
FCT-105T		646.09	5.0	33	38	120
NAS-37		527.13	0.015	1.4	10	5
NFM-33		569.22	0.063	23	-	-

Table 10: Calculated IC$_{50}$ values for inhibitors of different series, with activity against all used enzymes, expressed in µM, measured using enzymatic assay.
Symbol (-) represents the fact that IC$_{50}$ value was not measured or calculated.

As we can see, aromatized benzothiazole moiety seems to have better topo IV potential than tetrahydro-substituent (see KMG series versus THT-19; KSK-25), as well as [(1*H*-pyrrol-2-yl)carbonyl]amino moiety attached in 2-position instead of 6-position of benzothiazole. Interesting example is inactivity of KMG-31-33 against all the enzymes except of *E. coli* gyrase, in opposition to KMG-9,11,15,17 which are the active inhibitors of all tested enzymes. In addition, dichloro-substituted pyrrole core in compounds KMG-15 and KMG-17 manifest even better activity against both topo IV enzymes. IC$_{50}$ values of carboxylic acids are lower than of esters (THT-19 vs. KSK-25; TCF-4b vs. TCF-3b), possibly due to the differences in solubility.

When comparing TCF series, we can see that 4-bromo-5-methyl substitution of pyrrole core is sufficient, while 3,4-dibromo-5-methyl substitution is redundant and leads to lack of topo IV activity. On the contrary, 3,4-dichloro-5-methyl (TNH-10) or 3-bromo-4-chloro-5-methyl (TMK-16) substitution seems to have good influence at least for *S. aureus* topo IV activity.

Other options of modification could be 3-substituted benzoylamino (NFM-33) or phenylamino moiety (NAS-37) attached to the core in position 4. Calculated IC_{50} values are quite promising for those compounds, as well.

Table 11 shows IC_{50} values only for *E. coli* gyrase, other enzymes has not been measured yet.

Cmpd	Structure	MW [g/mol]	IC_{50} [µM] *E. coli* Gyrase	IC_{50} [µM] *S. aureus* Gyrase	IC_{50} [µM] *E. coli* Topo IV	IC_{50} [µM] *S. aureus* Topo IV
TKA-12a		520.20	2.3	-	-	-
TKA-15		506.17	0.89	-	-	-
TKA-16		520.20	4.5	-	-	-
TKA-17		492.14	1.1	-	-	-
TKA-25		498.21	6.8	-	-	-
TKA-26		423.33	1.9	-	-	-
NNS-18		400.21	0.19	-	-	-
NNS-19		442.29	2.2	-	-	-
NNS-20		384.21	4.0	-	-	-

Cmpd	Structure	MW [g/mol]	IC$_{50}$ [μM] E. coli Gyrase	IC$_{50}$ [μM] S. aureus Gyrase	IC$_{50}$ [μM] E. coli Topo IV	IC$_{50}$ [μM] S. aureus Topo IV
NNS-21		428.27	0.062	-	-	-
NNS-22		370.19	0.43	-	-	-
NNS-23		414.24	0.93	-	-	-

Table 11: Calculated IC$_{50}$ values for *E. coli* Gyrase inhibition of TKA and NNS series, expressed in μM, measured using enzymatic assay. *Inhibition of other types of enzymes was not measured, represented as (-) symbol.*

Given representatives of TKA series consist of [(4,5-dibromo-1*H*-pyrrol-2-yl)carbonyl]amino basic moiety, or in case of TKA-26 (3,4-dichloro-5-methyl-1*H*-pyrrol-2-yl)carbonyl]amino moiety attached to 2/6-position, respectively, of (tetrahydro-1,3-benzothiazol-2/6-yl)amino-structure further substituted with 3-oxocarboxylic acid, ester or methanesulfonamide. The 3,4-dichloro-5-methyl-substituted pyrrole core (TKA-26) appears to be preferable than 4,5-dibromo-substitued pyrrole core (TKA-25).

Benzoylamino-substituted NNS series is slightly better, but still comparable with TKA series. As before, 3,4-dichloro-5-methyl-substitution of pyrrole core seems promising. Again, for both TKA and NNS series, acids are more active than esters. However, further comparison cannot be done due to lack of other data.

Table 12 demonstrates IC$_{50}$ values of FCT series. Mostly, those compounds showed activity only for *E. coli* gyrase.

Cmpd	Structure	MW [g/mol]	IC$_{50}$ [μM] E. coli Gyrase	IC$_{50}$ [μM] S. aureus Gyrase	IC$_{50}$ [μM] E. coli Topo IV	IC$_{50}$ [μM] S. aureus Topo IV
FCT-217		624.24	0.52	*inactive*	*inactive*	*inactive*
FCT-218		610.22	1.7	*inactive*	*inactive*	*inactive*

Cmpd	Structure	MW [g/mol]	IC$_{50}$ [μM] *E. coli* Gyrase	IC$_{50}$ [μM] *S. aureus* Gyrase	IC$_{50}$ [μM] *E. coli* Topo IV	IC$_{50}$ [μM] *S. aureus* Topo IV
FCT-219		565.22	0.45	*inactive*	*inactive*	*inactive*
FCT-227		416.07	**inactive**	-	-	-
FCT-230		549.22	8.1	-	-	-
FCT-232		535.19	2.4	-	-	-
FCT-233		551.19	1.2	*inactive*	*inactive*	*inactive*
FCT-234		610.22	0.63	*inactive*	*inactive*	*inactive*
FCT-235		549.22	0.83	*inactive*	*inactive*	*inactive*
FCT-236		535.19	41	*inactive*	*inactive*	*inactive*
FCT-237		549.22	13	79	*inactive*	*inactive*

Table 12: Calculated IC$_{50}$ values for inhibitors of FCT series, expressed in μM, measured using enzymatic assay. *Symbol (-) represents the fact that IC$_{50}$ value was not measured or calculated*.

Listed FCT-series compound were inactive against *S. aureus* gyrase and both *E. coli* and *S. aureus* topo IV. Since FCT-227 was inactive even against *E. coli* gyrase, we can say that 4-aminobenzoic acid or (4-aminomethylbenzoic acid) is essential for its function. Also, substituted phenyl ring (4-hydroxyphenyl or 3-nitro-4-hydroxyphenyl) attached to 3-position of 1-oxopropyl seems to be more efficient then non-substituted ring (see e.g. FCT-219,234 vs. FCT-230,236).

4.2 ITC

For selected compounds listed in Table 13, ITC experiment was carried out as complementary method of evaluation. Binding thermodynamic parameters with inhibitor and *E. coli* Gyrase only were tested.

Cmpd	*Structure*	*MW* [g/mol]	IC$_{50}$ [µM] *E. coli* Gyrase	K_d [µM]	*ΔH* [kJ/mol]	*TΔS* [kJ/mol]
KSK-15		506.17	0.069	0.068	-59.6	-18.6
KSK-21		492.14	0.058	0.17	-48.2	-9.5
NFM-1		386.04	~ 0.1	0.75	-11.9	-23.0[a]
NHM-96b		485.09	0.36	0.11	-63.7	-24.0[c]
NHM-80		524.16	0.86	0.29	-51.6	-14.3[a]
NZ-105		445.07	0.450	0.050	-78.7	-37.1
TAK-8		471.31	0.064	0.48	-21.2	14.8[a]
TAK-10		416.32	0.21	0.95	-15.7	18.7[a]
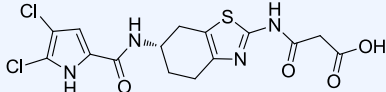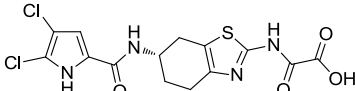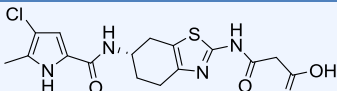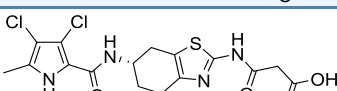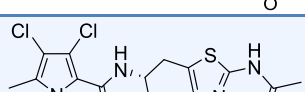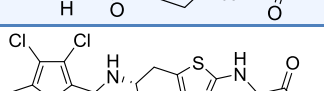
Cmpd	Structure	MW [g/mol]	IC$_{50}$ [μM] E. coli Gyrase	K$_d$ [μM]	ΔH [kJ/mol]	TΔS [kJ/mol]
THT-20		417.26	0.12	0.19	-63.5	-25.1
THT-21		403.23	0.59	0.26	-53.5	-15.9
TJL-6		396.85	0.12	0.14	-49.5	-17.3
TJL-19		431.29	0.022	0.077	-36.0	4.7
TNH-8		387.28	0.48	4.1	-5.3	26.3[b]
TNH-10		417.26	0.025	0.037	-60.3	-17.8

Table 13: Results obtained from ICT experiment performed for selected compounds. Results are expressed as dissociation constant K$_d$ [μM], enthalpy ΔH [kJ/mol] and entropy contribution to Gibbs energy -TΔS [kJ/mol]. IC$_{50}$ value for *E. coli* gyrase is also stated for illustration.

a – measured with 3% DMSO

b – measured with 1.5% DMSO

c – measured with 0.75% DMSO

Negative ΔG means spontaneous binding process; binding becomes tighter with more negative ΔG value. Although the binding affinity is the same (ΔG), total Gibbs energy can be actually expressed by different rate of entropy and enthalpy change, hence different binding mechanism. While more favourable (negative) ΔH reflects non-covalent interactions, such as hydrogen bonds, ΔS can be expressed as conformational entropy or solvation entropy (bound solvent released by hydrophobic groups). Sometimes, binding predictions are only considered due to ΔG, which can lead to wrong conclusions.

According to these premises, TAK-8, TAK-10 or TNH-8 show higher entropy contribution (lack of carboxylic group leads to hydrophobic interactions) while KSK, NHM, THT-series compounds are enthalpy favoured (established hydrogen bonds) or both enthalpy and entropy favoured. However, further thorough testing should be done to verify our deduction.

Solubility of compound was one of the problems we had to deal with while running the ITC experiment. In some cases, we had to use up to 3% DMSO to dissolve them properly, which is reflected in the results. Table 14 shows differences caused by presence of DMSO in the sample.

Cmpd	IC$_{50}$ [μM] E. coli Gyrase	K$_d$ [μM]	ΔH [kJ/mol]	TΔS [kJ/mol]	K$_d$ [μM] 3% DMSO	ΔH [kJ/mol] 3% DMSO	TΔS [kJ/mol] 3% DMSO
KSK-15	0.069	0.068	-59.6	-18.6	0.098	-64.2	-24.3
KSK-21	0.058	0.17	-48.2	-9.5	0.23	-49.3	-11.4
NZ-105	0.450	0.050	-78.7	-37.1	0.15	-94.0	-55.0
THT-20	0.12	0.19	-63.5	-25.1	0.25	-66.9	-29.2
THT-21	0.59	0.26	-53.5	-15.9	0.45	-57.8	-21.6
TJL-19	0.022	0.077	-36.0	4.7	0.16	-44.2	5.4
TJL-6	0.12	0.14	-49.5	-17.3	0.31	-54.7	-17.5

Table 14: Differences in measured parameters caused by 3% DMSO, shown in the right side.

As we can see, differences are obvious; all the measured parameters are significantly higher after addition of 3% DMSO. This phenomenon should be considered while solvating the compounds and if possible, avoided or minimized.

5 Discussion

Topoisomerase inhibitors based on pyrrolamide structure are subjects of several researches. [41,42] Characterization of Gyrase inhibitors builds on already ongoing Marex project of searching for novel gyrase B inhibitors, carried out at Faculty of Pharmacy, University of Ljubljana, based on clatrodin lead. Since *in vitro* evaluation is the first step of describing efficiency of synthesized compounds, even negative results are necessary; because of them, we can eliminate wrong assumptions and avoid them in the future. We were able to eliminate several series of compounds (data not shown) and focus on those with bigger potential. From this point of view, our work was successful, the aim was fulfilled and it provided the basis for the future project, which will be continued thanks to Innovative Training Network (ITN) by Marie Skłodowska-Curie Actions.

Several problems occurred during experiments. The biggest complication was a problematic solubility of compounds. It was proved that DMSO significantly affects the results; therefore its concentration should not be higher than 10% (enzymatic assay) or 3% (ITC), preferable even lower, if possible. Its influence was the most obvious in ITC experiment. Also, used enzyme concentrations were low and prone to errors [39]. Those are the reasons why we do not have enough sufficient data.

The limitation of enzymatic assay was its accuracy requirement. Supercoiling assays for *E. coli* and *S. aureus* gyrase were achievable more easily than relaxing assays for topo IV. While in the first case positive-negative control ratio varied between 1:8 to 1:11 (very satisfying), ratio for topo IV assays was an average of around 1:4 and inclined to bigger errors and unfavourable background signals.

During the evaluation, we determined several very potent compounds with IC_{50} in nM scale and some suitable dual inhibitors – KMG-15, KMG-17, NAS-37. Compounds from Table 11 showed very good results in *E. coli* GyrB inhibition; however, more data are needed to further evaluation. FCT series was satisfying in *E. coli* GyrB inhibition but unsuitable for dual targeting (GyrB/ParE inhibition). My suggestions for future *in vitro* evaluation are to finish enzymatic assays for all prepared compounds and to continue with microbiological testing to obtain additional data about membrane permeation etc.

ITC testing showed character of binding between the protein and inhibitor, which can be used in the future drug design strategies. Admittedly, further testing is needed, possibly also using other methods, such as X-ray crystallography for complete characterization of binding mechanism.

As mentioned before, other novel GyrB inhibitors will be synthesized and *in vitro* evaluated within ITN programme in following years.

6 Conclusion

DNA topoisomerases, specifically gyrase and topoisomerase IV as representatives of type II bacterial topoisomerases, are good targets for an enzymatic inhibition. Their blocking leads to the fault in essential cell functions and bacterial death without the possibility of multiplication. We evaluated several series of novel topoisomerase inhibitors with GyrB/ParE mechanisms. We used enzymatic assay for IC_{50} evaluation and ITC for thermodynamics characterization. Compounds KMG-15, KMG-17 and NAS-37 were most active dual targeting inhibitors with activity against all used enzymes. Compounds TJL-19, TMK-16, KMG-9 or KMG-11 showed as very potent against *E. coli* Gyrase but with average or not-measured activity against other enzymes. Further testing and additional experiments using different methods are needed to complete the characterization of novel inhibitors.

List of Tables

List of Figures

List of Schemes

References

1. BATES, Andrew D; MAXWELL, Anthony. *DNA topology*. 2nd ed. Oxford: Oxford University Press, 2005. ISBN 978-0-1915-4658-7.

2. ALBERTS, Bruce. *Essential cell biology*. 4th ed. New York: Garland Science, c2014, xxiii, 726, [112] s. ISBN 978-0-8153-4454-4.

3. LODISH, Harvey F. *Molecular cell biology*. 7th ed. New York: W.H. Freeman, c2013, [1244] s. ISBN 978-1-4641-0981-2.

4. DNA. *Wikipedia: the free encyclopedia.* [online]. 2001- [cit. 2015-01-23]. Accessible from: http://en.wikipedia.org/wiki/DNA.

5. Structure of the Double Helix. *GeneEd.* [online]. 2012- [cit. 2015-04-12]. Accessible from: http://geneed.nlm.nih.gov/topic_subtopic.php?tid=15&sid=16.

6. Sekundární struktura DNA. *WikiSkripta.* [online]. 2008- [cit. 2015-01-23]. ISSN 18046517. Accessible from:
http://www.wikiskripta.eu/index.php?title=Sekundární_struktura_DNA&oldid=283955.

7. PRATT, Charlotte W; CORNELY, Kathleen. *Essential biochemistry*. 3rd ed. Hoboken: Wiley, c2014, xxviii, 681, [30] s. ISBN 978-1-118-08350-5.

8. Plazmid. *WikiSkripta.* [online]. 2008-. [cit. 2015-04-12]. ISSN 18046517. Accessible from: http://www.wikiskripta.eu/index.php?title=Plazmid&oldid=286431.

9. DNA and Improtance of Proteins. *Biology Discussion.* [online] 2013- [cit. 2015-04-12]. Accessible from: http://www.biologydiscussion.com/molecular-biology/dna-and-importance-of-proteins-molecular-biology/1874.

10. FELSENFELD, Gary; GROUDINE, Mark. Controlling the double helix. *Nature* [online]. 2003, vol. 421, issue 6921, s. 448-453 [cit. 2015-05-10]. DOI: 10.1038/nature01411.

11. MIRKIN, Sergei M. DNA Topology: Fundamentals. *eLS* [online]. May 2001, John Wiley & Sons Ltd, Chichester. DOI: 10.1038/npg.els.0001038. Accessible from: http://www.els.net.

12. WATSON, James D. *Molecular biology of the gene*. 6th ed. San Francisco: Pearson, c2008, xxxii, 841 s. ISBN 978-0-321-50781-5.

13. BARANELLO, Laura; KOUZINE, Fedor; LEVENS, David. DNA Topoisomerases: Beyond the standard role. *Transcription*, 2013, 4.5: 232-237.

14. FORTERRE, Patrick, et al. Origin and evolution of DNA topoisomerases. *Biochimie*, 2007, 89.4: 427-446.

15. ROCA, Joaquim. The mechanisms of DNA topoisomerases. *Trends in biochemical sciences*, 1995, 20.4: 156-160.

16. CHAMPOUX, James J. DNA topoisomerases: structure, function, and mechanism. *Annual review of biochemistry*, 2001, 70.1: 369-413.

17. RAJAN, Rakhi, et al. Identification of one of the apurinic/apyrimidinic lyase active sites of topoisomerase V by structural and functional studies. *Nucleic acids research*, 2013, 41.1: 657-666.

18. FORTERRE, Patrick. DNA topoisomerase V: a new fold of mysterious origin. *Trends in biotechnology*, 2006, 24.6: 245-247.

19. BATES, Andrew D.; MAXWELL, Anthony. DNA topology: topoisomerases keep it simple. *Current Biology*, 1997, 7.12: R778-R781.

20. LEVINE, Cindy; HIASA, Hiroshi; MARIANS, Kenneth J. DNA gyrase and topoisomerase IV: biochemical activities, physiological roles during chromosome replication, and drug sensitivities. *Biochimica et Biophysica Acta (BBA)-Gene Structure and Expression*, 1998, 1400.1: 29-43.

21. BATES, Andrew D. DNA topoisomerases: single gyrase caught in the act. *Current biology*, 2006, 16.6: R204-R206.

22. REECE, Richard J.; MAXWELL, Anthony; WANG, James C. DNA gyrase: structure and function. *Critical reviews in biochemistry and molecular biology*, 1991, 26.3-4: 335-375.

23. NÖLLMANN, Marcelo; CRISONA, Nancy J.; ARIMONDO, Paola B. Thirty years of Escherichia coli DNA gyrase: from in vivo function to single-molecule mechanism. *Biochimie*, 2007, 89.4: 490-499.

24. COUTURIER, Martine; BAHASSI, El Mustapha; VAN MELDEREN, Laurence. Bacterial death by DNA gyrase poisoning. *Trends in microbiology*, 1998, 6.7: 269-275.

25. ALDRED, Katie J.; KERNS, Robert J.; OSHEROFF, Neil. Mechanism of quinolone action and resistance. *Biochemistry*, 2014, 53.10: 1565-1574.

26. MITTON-FRY, Mark J., et al. Novel quinoline derivatives as inhibitors of bacterial DNA gyrase and topoisomerase IV. *Bioorganic & medicinal chemistry letters*, 2013, 23.10: 2955-2961.

27. DRLICA, Karl. Mechanism of fluoroquinolone action. *Current opinion in microbiology*, 1999, 2.5: 504-508.

28. HARTL, Jiří. *Farmaceutická chemie IV.* 2., nezměn. vyd. Praha: Karolinum, 2012, 166 s. ISBN 978-80-246-2129-6.

29. HYNIE, Sixtus. *Speciální farmakologie Díl VII/B: Protiinfekční léčiva.* Praha: Karolinum, 1998. 140 s. ISBN 80-7184-783-6.

30. HEIDE, Lutz. New aminocoumarin antibiotics as gyrase inhibitors. *International Journal of Medical Microbiology*, 2014, 304.1: 31-36.

31. HYNIE, Sixtus. *Speciální farmakologie Díl VII/A: Protinádorová chemoterapeutika a imunomodulační látky*. Praha: Karolinum, 1998. 140 s. ISBN 80-245-0656-9.

32. GLASER, Bryan T., et al. A high-throughput fluorescence polarization assay for inhibitors of gyrase B. *Journal of biomolecular screening*, 2011, 16.2: 230-238.

33. MAXWELL, Anthony; BURTON, Nicolas P.; O'HAGAN, Natasha. High-throughput assays for DNA gyrase and other topoisomerases. *Nucleic acids research*, 2006, 34.15: e104-e104.

34. BURRELL, Matthew R.; BURTON, Nicolas P.; MAXWELL, Anthony. A high-throughput assay for DNA topoisomerases and other enzymes, based on DNA triplex formation. In: *Drug-DNA Interaction Protocols*. Humana Press, 2010. p. 257-266.

35. ANDERLE, Christine, et al. Biological activities of novel gyrase inhibitors of the aminocoumarin class. *Antimicrobial agents and chemotherapy*, 2008, 52.6: 1982-1990.

36. Technical information. *Inspiralis*. [online]. 2006- [cit. 2015-04-12]. Accessible from: http://www.inspiralis.com/go/technical_information.php.

37. VELÁZQUEZ-CAMPOY, Adrián, et al. Isothermal titration calorimetry. *Current Protocols in Cell Biology*, 2004, 17.8. 1-17.8. 24.

38. LAFITTE, Daniel, et al. DNA gyrase interaction with coumarin-based inhibitors: the role of the hydroxybenzoate isopentenyl moiety and the 5'-methyl group of the noviose. *Biochemistry*, 2002, 41.23: 7217-7223.

39. Nano ITC. *TA Instruments.* [online]. 2015- [cit. 2015-04-12]. Accessible from: http://www.tainstruments.com/main.aspx?id=263&n=1&siteid=11.

40. JELESAROV, Ilian; BOSSHARD, Hans Rudolf. Isothermal titration calorimetry and differential scanning calorimetry as complementary tools to investigate the energetics of biomolecular recognition. *Journal of molecular recognition*, 1999, 12.1: 3-18.

41. SHERER, Brian A., et al. Pyrrolamide DNA gyrase inhibitors: optimization of antibacterial activity and efficacy. *Bioorganic & medicinal chemistry letters*, 2011, 21.24: 7416-7420.

42. URIA-NICKELSEN, Maria, et al. Novel DNA gyrase inhibitors: Microbiological characterisation of pyrrolamides. *International journal of antimicrobial agents*, 2013, 41.1: 28-35.

Appendix 1

The examples of the table layout for enzymatic assay, raw data and recalculation of results are shown.

	1	2	3	4	5	6	7	8	9	10	11	12
A	TNH-10 1 µM	NAS-37 1 µM	NAS-39 1 µM	NHM-80 40 µM	NFM-33 40 µM	NAS-29 100 µM	TAK-8 4 µM	TAK-10 4 µM	SJG-13a 100 µM	SJG-13a 10 µM	FCT-218 10 µM	FCT-218 1 µM
B	TNH-10 0,38 µM	NAS-37 0,38 µM	NAS-39 0,38 µM	NHM-80 15 µM	NFM-33 15 µM	NAS-29 37,5 µM	TAK-8 1,5 µM	TAK-10 1,5 µM	AGP-72 100 µM	AGP-72 10 µM	FCT-230 10 µM	FCT-230 1 µM
C	TNH-10 0,14 µM	NAS-37 0,14 µM	NAS-39 0,14 µM	NHM-80 5,6 µM	NFM-33 5,6 µM	NAS-29 14,1 µM	TAK-8 0,56 µM	TAK-10 0,56 µM	TTM-56 100 µM	TTM-56 10 µM	FCT-232 10 µM	FCT-232 1 µM
D	TNH-10 0,053	NAS-37 0,053	NAS-39 0,053	NHM-80 2,11 µM	NFM-33 2,11 µM	NAS-29 5,27 µM	TAK-8 0,21 µM	TAK-10 0,21 µM	FCT-216 100 µM	FCT-216 10 µM	FCT-234 10 µM	FCT-234 1 µM
E	TNH-10 0,020	NAS-37 0,020	NAS-39 0,020	NHM-80 0,79 µM	NFM-33 0,79 µM	NAS-29 1,98 µM	TAK-8 0,08 µM	TAK-10 0,08 µM	FCT-219 100 µM	FCT-219 10 µM	FCT-235 10 µM	FCT-235 1 µM
F	TNH-10 0,0074	NAS-37 0,0074	NAS-39 0,0074	NHM-80 0,30 µM	NFM-33 0,30 µM	NAS-29 0,74 µM	TAK-8 0,03 µM	TAK-10 0,03 µM	FCT-222 100 µM	FCT-222 10 µM	KMG-31 1 µM	KMG-31 0,1 µM
G	TNH-10 0,0028	NAS-37 0,0028	NAS-39 0,0028	NHM-80 0,11 µM	NFM-33 0,11 µM	NAS-29 0,28 µM	TAK-8 0,011	TAK-10 0,011	FCT-226 100 µM	FCT-226 10 µM	KMG-32 1 µM	KMG-32 0,1 µM
H	0 %	0 %	NOVOB 0,2 µM	NOVOB 0,2 µM	NOVOB 0,1 µM	NOVOB 0,1 µM	100 %	100 %	FCT-217 10 µM	FCT-217 1 µM	KMG-33 1 µM	KMG-33 0,1 µM

Table 15: Table layout of enzymatic assay [2014-11-06]. Layout corresponds with 96-well microtitre plate.

Wells *H1-8* represent control panel, using novobiocin as reference compound. Columns *1-8* are, in this case, prepared for IC$_{50}$ evaluation (wide range of concentration of one compound), with 0.375 as dilution factor. Columns *9-12* are set up for screening (two different concentrations of one compound, usually with factor 10). Compound preparation was made prior to each experiment, compound were stored in stock concentrations (diluted in DMSO) at -18 °C.

Table 16 shows raw data get using mentioned software. Numbers represents absolute values of measured fluorescence, additionally interpreted by colour shade. The darker the blue shade is the higher fluorescence was measured.

	1	2	3	4	5	6	7	8	9	10	11	12
A	1136	1155	1435	973	943	1814	1105	1067	7238	8945	1278	5953
B	1313	1087	1784	1106	1018	2767	1156	1543	1545	2719	1556	9717
C	2766	1382	3913	1058	998	2079	3715	2942	13628	13579	1640	9830
D	6035	2832	6118	1452	1052	7876	7389	7785	10239	5976	1282	5931
E	8152	5259	8457	8826	984	7408	10008	10805	1118	1100	1009	6228
F	8250	7496	7856	8875	1080	10466	13014	11223	13750	13691	956	6458
G	9329	9715	10439	10538	1860	11485	11131	12764	1534	3053	6104	12014
H	946	1005	2351	2309	3834	6104	11622	11545	1061	9520	3328	9831

Table 16: Raw data – absolute values of fluorescence [2014-11-06]. The layout corresponds with Table 15.

Absolute values were recalculated to more readable form as percentage of inhibition (Table 17). Relationship

$$I = \frac{measured\ value - blank}{I_{MAX} - blank} \cdot 100 \qquad (10)$$

was used, where I [%] stands for rate of total inhibition, I_{MAX} is average of values *H7-H8* and **blank** is average of values *H1-H2*.

	1	2	3	4	5	6	7	8	9	10	11	12
A	2	2	4	0	0	8	1	1	59	75	3	47
B	3	1	8	1	0	17	2	5	5	16	5	82
C	17	4	28	1	0	10	26	19	119	119	6	83
D	48	18	48	4	1	65	60	64	87	47	3	47
E	68	40	71	74	0	61	85	93	1	1	0	50
F	69	61	65	74	1	89	113	97	120	120	0	52
G	79	82	89	90	8	99	96	111	5	20	48	104
H	0	0	13	13	27	48	100	100	1	81	22	83

Table 17: Percentage of inhibition [2014-11-06]. Layout corresponds with Table 15. Range of values is derived from the assumption that 0% ~ total inhibition; 100% ~ no inhibition.

Appendix 2

The example of ITC output is shown. Each peak on the first graph corresponds with one injection of ligand to sample cell with enzyme. Area under the curve is then integrated and fitted into the curve illustrated in the second part of the picture.
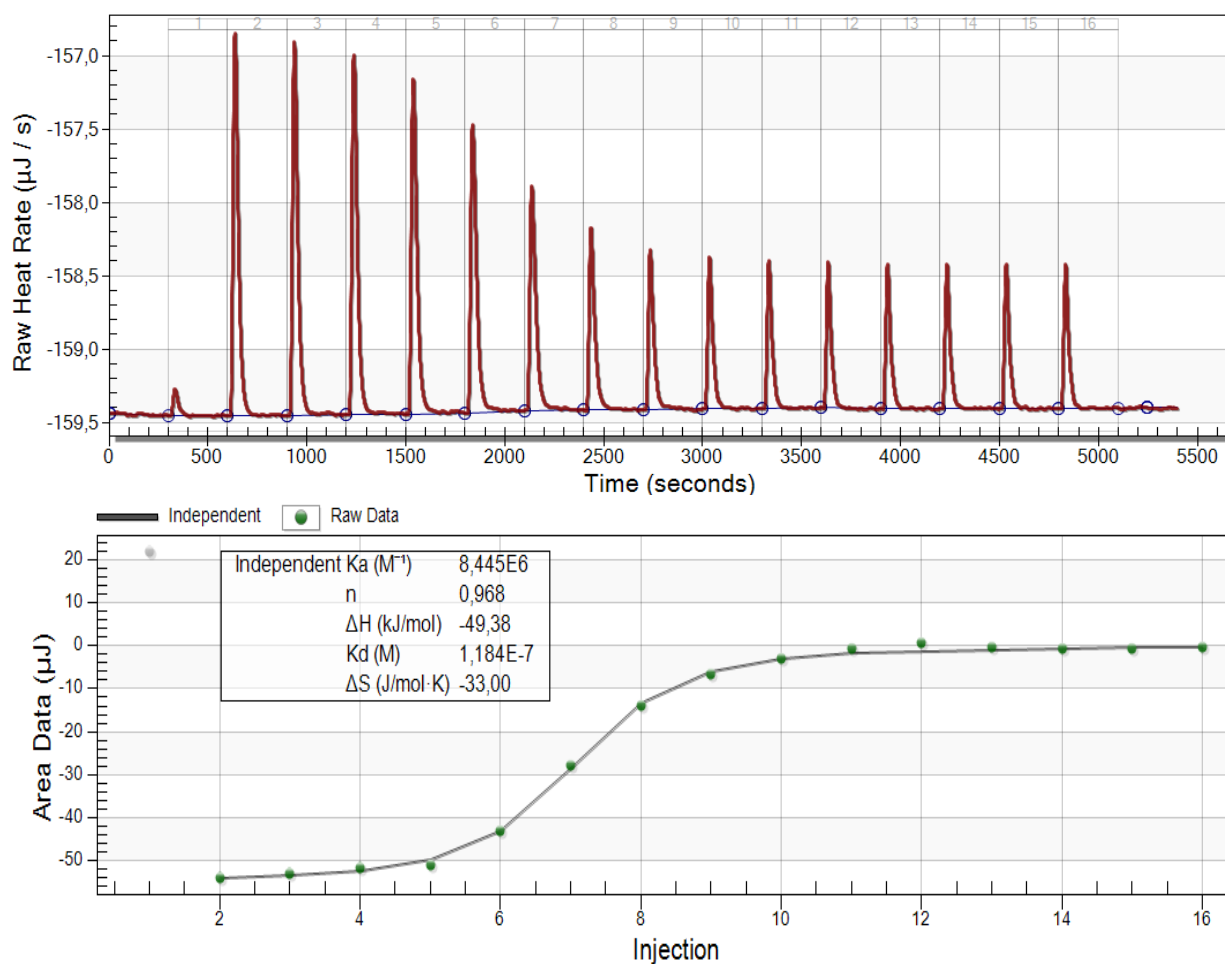

Figure 9: Illustration of results obtained by NanoAnalyze software. This particular graph belongs to compound TJL-6.

After curve correlation, an independent model is calculated and required parameters are obtained.